Evaluating of melting-ice process in a vertical pipe with consideration of net sensible heat

Hung Thanh Nguyen [1*], Eirik Gjerløw[1] and Minh-Thu T. Huynh[2*]

[1] *UiT the Arctic University of Norway - IVT. Fak. – Institute of Building, Energy and Material Technology*
[2] *Ho Chi Minh City University of Technology and Education – Faculty of Vehicle and Energy Engineering*
[*] *Corresponding authors: thuhtm@hcmute.edu.vn*

Abstract. In ice-melting process, motion of liquid-solid interface is complicated due to moving boundary, which is also called Stefan interface problem. Although the Stefan model has been widely utilized, it frequently overestimates the melting rate. In the present study, the net-sensible-heat of the phases are taken into account as an additional physical effect to the Stefan model for one-phase case and two-phase cases. The proposed model applied differential forms of energy conservations for each phase and the whole system with a practical or engineering approach. For the particular case of an ice-melting process in a vertical pipe, the results showed that, for the one-phase case, the migration of the interface of the proposed model was lowered by 18.5%, 12.0% and 4.3% compared to the Stefan model, Neumann solution and "modified Berggren Equation", respectively, after a simulation period of 25 days. For the two-phase case, a similar trend of interface migration was achieved for the proposed and Stefan models. The former was approximately 11.4% lower than the latter after about 12 days, following this the difference between the models thereafter remains stable for the remainder of the simulation period. Additionally, the proposed model's sensitivity is also examined by varying the inputs of surface temperature, initial temperature, and pipe-length change. It was observed that the coefficients of proportionality of the proposed models and relevant models have reasonable agreement.

Keywords: Stefan model, melting process, interface condition, melt-front position, sensible heat.

1. Introduction

Ice formation and melting problems are important considerations in Arctic regions, for instance in sea ice formation along Arctic shipping routes (Li et al. 2021) and thawing processes in seasonally frozen ground (Sveen et al. 2017). The Stefan equations have commonly been applied to calculate the rate of melting and freezing of ice (Fox 1992). The Stefan models and the Stefan free boundary problems were originally presented in 1889 by Josef Stefan. He contributed four significant papers on the kinetic theory of heat, these were on the heat conduction in fluids (Stefan 1889a), diffusion in fluids (Stefan 1889b) ice formation (Stefan 1889c) and evaporation (Stefan 1889d). These papers present the mathematics and physical models of the time-moving interface (free boundary conditions and moving boundary problem). These models are often called the ''Stefan problem'' and ''Stefan interface condition''.

The original Stefan problem treats the formation of ice in the polar seas (Stefan 1889c). The Stefan interface condition models consider a quantity of seawater which is cooled down to its freezing temperature. Thereafter the air temperature does not change, and the ice layer will grow as a function of time. According to this model the thickness of the ice layer is proportional to the square root of time. Nowadays, a large class of moving boundaries has been referred to as Stefan problems. For instance, the models are relevant for predicting the freezing front in water saturated porous materials (Berggren 1943) and the Stefan models are also frequently applied as an approach for predicting the thickness of the active layer in permafrost (Jumikis 1977, French 2007, Kurylyk 2015, Kurylyk et al. 2014, Changwei and Gough 2013, Hayashi et al. 2007). The Stefan interface conditions are based on the conservation of energy at the interface with the following assumptions: (i) the density of water and ice are the same, (ii) the moving boundary is

affected by heat flux of liquid for one-phase case and by net heat flux of liquid and solid phases in two-phase case. Therefore, the Stefan model can over-estimate the motion of the interface of phase change problems (Alexiades and Solomon, 1993). In efforts to improve the solution, additional physical parameters have been considered. For instance, the Neumann solution (Neumann 1860), known as analytical exact solution, has accounted for the sensible heat and the solution was implicit. Aldrich and Paynter (1953) accounted for the influence of sensible heat by a correction factor to the Stefan equations, which is also called the "Modified Berggren Equation". In the study of Glass et al. (Glass et al. 1991), the authors have formulated and given numerical solutions to the hyperbolic Stefan problems with consideration of sensible heat. The Darcy-Stefan model was coupled with the porous elastic equation to investigate the thawing process (Deng et al. 2019). However, these studies were quite complicated, and applying them to practical problems has been challenging for engineers. Thus, based on the Neumann solution, Kurylyk and Hayashi (Kurylyk and Hayashi, 2016) have proposed new correction factor equations by fitting polynomial functions, which consider non-zero initial temperatures of the solid phase. In addition, the effects of volume change have been included in the model by adding the total thermal balance (Rodrıguez-Aleman et al., 2020). Their study has considered an important effect due to density difference to the migrating of the interface in PCM. Besides, the prediction of the moving interface also was examined with uniform volumetric energy generation (Chan and Hsu 1987, Crepeau and Siahpush 2012, An and Su 2013).

In short, the advantage of the Stefan equations, their simplicity, should be maintained but the solution needs to be improved by including more physical parameters. In the present paper, the interface conditions are developed to include the net-sensible-heat of the phases in the differential conservation of energy equations. Particularly, the motion of the melt-front of the ice-melting process (ice-water) in a one-dimensional vertical pipe is investigated. In addition, they are compared with the Stefan models and other related studies. Finally, a sensitivity analysis, which varies input parameters (heat flux into the pipe in term of surface temperature, initial temperature, and pipe length), is performed on the models.

2. Methodology

In this section, the ice-melting process in a vertical pipe, whose length and cross section area are l and A respectively (sketched in *Figure 1)*, is investigated. The initial phase of ice-water inside the pipe is solid, at temperature T_i; for a semi-infinite pipe, this temperature is assumed to be equal to the temperature at the end of the pipe, T_l. Then the pipe is heated from the top with a constant surface temperature of T_0.

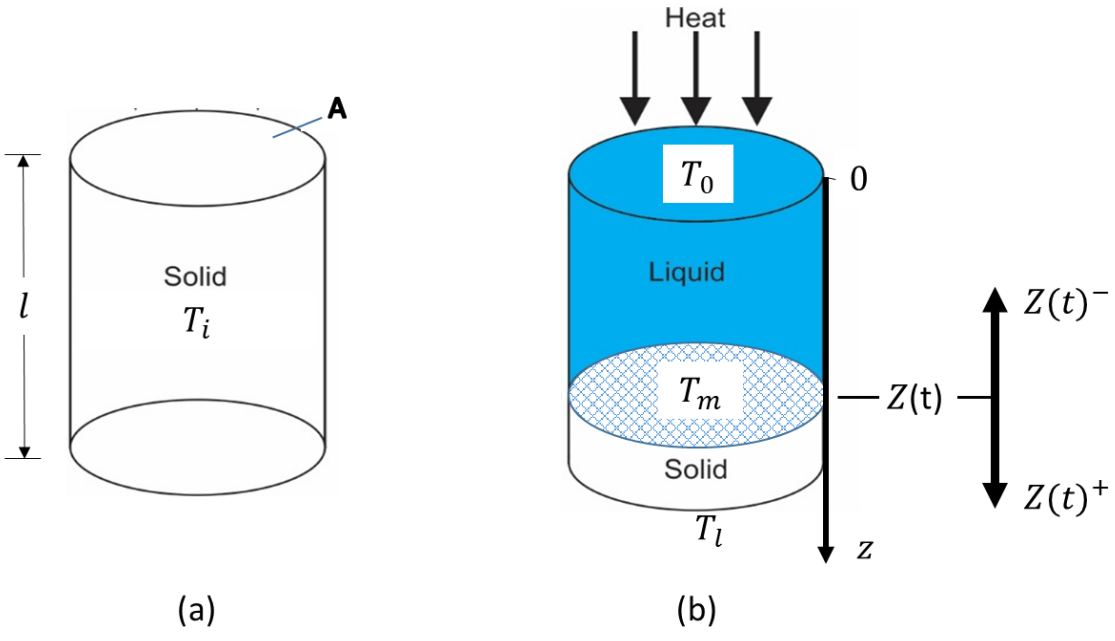

Figure 1. Melting ice-water in a vertical pipe: (a) Initial condition, $t = 0$; (b) During melting process, $t > 0$.

2.1 Stefan and related models for current scenario

With the assumption that the pipe is well-insulated, and that the heat transfer mechanism of conduction is dominant in one-dimension, the conservation of energy of the Stefan model in a semi-infinite pipe for each phase can be derived as following (Alexiades and Solomon 1993, Cannon et al. 1980):

- For the liquid region: $0 \leq z < Z(t), t > 0$:

$$Z(t)A\rho_L c_L \frac{\partial T(z,t)}{\partial t} = -A\lambda_L \frac{\partial T(0,t)}{\partial z} + A\lambda_L \frac{\partial T(Z^-,t)}{\partial z} \quad (1)$$

- For the solid region: $Z(t) < z \leq l, t > 0$

$$\big(l - Z(t)\big)A\rho_s c_s \frac{\partial T(z,t)}{\partial t} = -A\lambda_s \frac{\partial T(Z^+,t)}{\partial z} + A\lambda_s \frac{\partial T(l,t)}{\partial z} \quad (2)$$

- Initial conditions:

$$Z(0) = 0 \quad (3)$$

$$T(z,0) = T_i < T_m \quad (4)$$

- Boundary conditions:

At the top surface of the pipe: $T(0,t) = T_0 > T_m$ (5)

At the bottom surface of the pipe: $T_l = T_i, t > 0$ (6)

- Interface conditions:

$$T(Z,t) = T_m, t > 0 \quad (7)$$

At the control volume of the pipe as shown in *Figure 1*, the total enthalpy of ice-water at $t > 0$, referred to the melting temperature T_m, is calculated by (Alexiades and Solomon 1993, Tao 1979):

$$H(t) = A\left[\int_0^{Z(t)} [\rho_L c_L (T(z,t) - T_m) + \rho_L L]dz + \int_{Z(t)}^{l} \rho_s c_s (T(z,t) - T_m)dz\right] \quad (8)$$

By applying Leibniz integral rule (Alexiades and Solomon 1993), we obtain:

$$\frac{\partial H(t)}{\partial t} = A\left[\begin{aligned}&\rho_L c_L [T(Z(t),t) - T_m]\frac{\partial Z(t)}{\partial t} + \int_0^{Z(t)} \rho_L c_L \frac{\partial T(z,t)}{\partial t}dz \\ &+ \rho_L L\frac{\partial Z(t)}{\partial t} + \int_{Z(t)}^{l} \rho_s c_s \frac{\partial T(z,t)}{\partial t}dz - \rho_s c_s [T(Z(t),t) - T_m]\frac{\partial Z(t)}{\partial t}\end{aligned}\right] \quad (9)$$

By imposing $T(Z,t) = T_m$ from Eq. (7), the terms $\rho_L c_L [T(Z(t),t) - T_m]\frac{\partial Z(t)}{\partial t}$ and $\rho_s c_s [T(Z(t),t) - T_m]\frac{\partial Z(t)}{\partial t}$ are omitted. Hence, Eq. (9) can be reduced to:

$$\frac{\partial H(t)}{\partial t} = A\left[\int_0^{Z(t)} \rho_L c_L \frac{\partial T(z,t)}{\partial t}dz + \rho_L L\frac{\partial Z(t)}{\partial t} + \int_{Z(t)}^{l} \rho_s c_s \frac{\partial T(z,t)}{\partial t}dz\right] \quad (10)$$

By substituting the heat conduction model for each phase Eqs. (1) – (2) into Eq. (10), it becomes:

$$\frac{\partial H(t)}{\partial t} = A\left[\left[-\lambda_L \frac{\partial T_L(0,t)}{\partial z} + \lambda_L \frac{\partial T_L(Z^-,t)}{\partial z}\right] + \rho_L L\frac{\partial Z(t)}{\partial t} + \left[-\lambda_s \frac{\partial T(Z^+,t)}{\partial z} + \lambda_s \frac{\partial T(l,t)}{\partial z}\right]\right] \quad (11)$$

On the other hand, the rate of change for energy in the whole pipe is balanced with the net heat flux into and leaving the pipe (Alexiades and Solomon 1993, Charach and Rubinstein 1991):

$$\frac{\partial H(t)}{\partial t} = A\left[-\lambda_L \frac{\partial T_L(0,t)}{\partial z} + \lambda_s \frac{\partial T(l,t)}{\partial z}\right] \quad (12)$$

By substituting Eq. (12) into Eq. (11), we obtain the interface condition as heat is transferred in both phases (liquid and solid), which is herein referred to as the two-phase Stefan interface condition:

$$\rho_L L \frac{\partial Z}{\partial t} = -\lambda_L \frac{\partial T}{\partial z}\Big|_{Z^-} + \lambda_s \frac{\partial T}{\partial z}\Big|_{Z^+} \quad (13)$$

When there is no-heat flux into the solid phase, which is herein referred to as the one-phase Stefan interface condition, Eq. (13) reduces to:

$$\rho_L L \frac{\partial Z}{\partial t} = -\lambda_L \frac{\partial T}{\partial z}\Big|_{Z^-} \quad (14)$$

By integrating Eq. (14), it yields the interface condition of one-phase Stefan:

$$\int_0^{Z(t)} z dz = \frac{\lambda_L (T_0 - T_m)}{\rho_L L} \int_0^t dt \rightarrow Z^2(t) = \frac{2\lambda_L (T_0 - T_m)}{\rho_L L} t$$

$$\rightarrow Z(t) = \sqrt{\frac{2\lambda_L (T_0 - T_m)}{\rho_L L}} \sqrt{t} \quad (15)$$

For the two-phase Stefan model, in which heat conduction in solid phase is considered, the pipe-length parameters, β, is introduced and defined:

$$l - Z(t) = \beta Z(t), \beta \in R \quad (16)$$

By replacing β and integrating Eq. (13), the interface condition is achieved:

$$\int_0^{Z(t)} \beta z dz = \frac{\beta\lambda_L (T_0 - T_m) - \lambda_s (T_m - T_l)}{\rho_L L} \int_0^t dt \rightarrow Z^2(t) = \frac{2[\beta\lambda_L (T_0 - T_m) - \lambda_s (T_m - T_l)]}{\beta \rho_L L} t$$

$$\rightarrow Z(t) = \sqrt{\frac{2[\beta\lambda_L (T_0 - T_m) - \lambda_s (T_m - T_l)]}{\beta \rho_L L}} \sqrt{t} \quad (17a)$$

Eq. (17a) is the solution to evaluate the migration of the interface of two-phase Stefan model.

Effects of thermodynamic equilibrium due to volume change in phase change

Beside the energy conservation equation as the above, Rodrıguez-Aleman et al. (2020) includes the effects of the thermodynamic equilibrium due to volume change during phase transition or density difference of the phases. In comparison to the solution of interface of the above Eq. (17a), the equilibrium interface position is achieved as:

$$Z_{eq}(t) = Z(t) + \left(\frac{1}{\rho_L} - \frac{1}{\rho_s}\right) \frac{\Delta U}{L} \quad (17b)$$

where $\Delta U = \rho_L c_L \int_0^{Z(t)} (T(z,t) - T_m) dz - \rho_s c_s \int_{Z(t)}^{l} (T(z,t) - T_m) dz$ is the total change of the internal energy between the state of the system at interface position $Z(t)$ as in Eq. (17a) and at thermodynamic equilibrium.

2.2 Proposed model.

In the present study, similar to the above Stefan model for a semi-infinite pipe, the total enthalpy of the model at time t, Eq. (8), can be simply rewritten as:

$$H(t) = c_L m_L(t) \Delta T_L(t) + m_L(t) L + c_s m_s(t) \Delta T_s(t) \quad (18)$$

However, instead of using the Leibniz integral rules to solve Eq. (8) as in Stefan's model, the differential equation of the conservation of energy for a control volume is used in the proposed model. The rate of change for $H(t)$ in the pipe is:

$$\frac{\partial H}{\partial t} = \frac{\partial (c_L m_L \Delta T_L)}{\partial t} + \frac{\partial (m_L L)}{\partial t} + \frac{\partial (c_s m_s \Delta T_s)}{\partial t}$$

$$= c_L \frac{\partial m_L}{\partial t} \Delta T_L + c_L m_L \frac{\partial \Delta T_L}{\partial t} + \frac{\partial m_L}{\partial t} L + c_s \frac{\partial m_s}{\partial t} \Delta T_s + c_s m_s \frac{\partial \Delta T_s}{\partial t} \quad (19)$$

Taking the cross-section area A out from the right-hand side, Eq. (19) becomes:

$$\frac{\partial H(t)}{\partial t} = A \begin{bmatrix} c_L \rho_L \frac{\partial Z(t)}{\partial t} \Delta T_L + c_L \rho_L Z(t) \frac{\partial \Delta T_L}{\partial t}\Big|_{z:0 \to Z^-} \\ + \rho_L \frac{\partial Z(t)}{\partial t} L + c_s \rho_s \frac{\partial (l - Z(t))}{\partial t} \Delta T_s + c_s \rho_s (l - Z(t)) \frac{\partial \Delta T_s}{\partial t}\Big|_{z:Z^+ \to l} \end{bmatrix} \quad (20)$$

By substituting the heat conduction models Eqs. (1) and (2), for each phase into Eq. (20), we obtain:

$$\frac{\partial H(t)}{\partial t} = A \begin{bmatrix} c_L \rho_L \frac{\partial Z(t)}{\partial t} \Delta T_L - \lambda_L \frac{\partial T(0,t)}{\partial z} + \lambda_L \frac{\partial T(Z^-,t)}{\partial z} \\ + \rho_L \frac{\partial Z(t)}{\partial t} L - c_s \rho_s \frac{\partial Z(t)}{\partial t} \Delta T_s - \lambda_s \frac{\partial T(Z^+,t)}{\partial z} + \lambda_s \frac{\partial T(l,t)}{\partial z} \end{bmatrix} \quad (21)$$

Equation (21) includes the term $c_L \rho_L \frac{\partial Z(t)}{\partial t} \Delta T_L$ and $c_s \rho_s \frac{\partial Z(t)}{\partial t} \Delta T_s$ which are representative of rate of sensible heat of liquid and solid phases, respectively; while they are omitted in Eq. (11).

After substituting Eq. (12) into Eq. (21) and rearranging we obtain:

$$c_L \rho_L \frac{\partial Z(t)}{\partial t} \Delta T_L + \rho_L \frac{\partial Z(t)}{\partial t} L - c_s \rho_s \frac{\partial Z(t)}{\partial t} \Delta T_s = -\lambda_L \frac{\partial T(Z^-,t)}{\partial z} + \lambda_s \frac{\partial T(Z^+,t)}{\partial z} \quad (22)$$

Similarly, for the one-phase case when there is no-heat flux into the solid phase, $\lambda_s T'_{z=Z(t)^+} = 0$, and it also has no sensible heat in the solid phase. For this case, Eq. (22) reduces to:

$$c_L \rho_L \frac{\partial Z(t)}{\partial t} \Delta T_L + \rho_L \frac{\partial Z(t)}{\partial t} L_s = -\lambda_L \frac{\partial T(Z^-,t)}{\partial z} \quad (23)$$

Then, integrating yields the following:

$$\int_0^{Z(t)} z dz = \frac{\lambda_L (T_0 - T_m)}{\rho_L L + c_L \rho_L \Delta T_L} \int_0^t dt \to Z^2(t) = \frac{2\lambda_L (T_0 - T_m)}{\rho_L L + c_L \rho_L \Delta T_L} t$$

$$\to Z(t) = \sqrt{\frac{2\lambda_L (T_0 - T_m)}{\rho_L L + c_L \rho_L \Delta T_L}} \sqrt{t} \quad (24)$$

Eq. (24) is the proposed interface condition for estimating melt-front migration in one-phase with the given scenario. For two-phase case, interface condition is estimated as follow:

$$\int_0^{Z(t)} \beta z dz = \frac{\beta \lambda_L (T_0 - T_m) - \lambda_s (T_m - T_l)}{\rho_L L + c_L \rho_L \Delta T_L - c_s \rho_s \Delta T_s} \int_0^t dt \to Z^2(t) = \frac{2[\beta \lambda_L (T_0 - T_m) - \lambda_s (T_m - T_l)]}{\beta (\rho_L L + c_L \rho_L \Delta T_L - c_s \rho_s \Delta T)} t$$

$$\to Z(t) = \sqrt{\frac{2[\beta \lambda_L (T_0 - T_m) - \lambda_s (T_m - T_l)]}{\beta (\rho_L L + c_L \rho_L \Delta T_L - c_s \rho_s \Delta T_s)}} \sqrt{t} \quad (25)$$

3. RESULTS AND DISCUSSIONS

In order to validate the interface conditions using the proposed methodology, we compare the results with those of previous related studies which are applicable for the given scenario for both one-phase and two-phase cases. For the one-phase case, beside Stefan the one-phase case, the Neumann solution and the "Modified Berggren Equation" are used as comparisons. On the other hand, for the two-phase case, the method proposed by Kurylyk and Hayashi

(Kurylyk and Hayashi, 2016) with non-zero initial ice temperature case and the effects of density difference to the migration of the interface (Rodrıguez-Aleman et al., 2020), are compared.

3.1. Results

The model of a vertical pipe in *Figure 1* with length l of 1.0 m is used. With the intention of simulating sensible heat in both solid and liquid phases, the initial temperature of the ice is $T_i = T_l = -10℃$ and it is then heated from the top to maintain the top surface temperature of $T_0 = 40℃$, which is used to boost the melting process. In this calculation, for simplification, it is assumed that:

(i) the initial conditions or first step of the two-phase cases is the same as those of the one-phase cases for Stefan model and the proposed model.
(ii) The increase in temperature: $\Delta T_L = T_0 - T_m$, $\Delta T_s = T_m - T_l$
(iii) The thermal properties of ice-water are unchanged; values are in Table 1.

TABLE 1. Thermal properties of ice and water [Cengel et al. 2006]

Thermal properties	Ice at temperature **0**℃	Water at temperature **0**℃
Density	$\rho_s = 920\ \mathrm{kg/m^3}$	$\rho_L = 1000\,\mathrm{kg/m^3}$
Specific heat	$c_s = 2040\ \mathrm{J/\ kg \cdot K}$	$c_L = 4217\ \mathrm{J/\ kg \cdot K}$
Thermal conductivity	$\lambda_s = 1.88\ \mathrm{W/\ m \cdot K}$	$\lambda_L = 0.569\ \mathrm{W/\ m \cdot K}$
Latent heat	$L = 333\,700\ \mathrm{J/kg}$	
Melting temperature	$T_m = 0℃$	

3.1.1. One-phase models

Figure 2 shows the results for the one-phase interface condition from different models to estimate the melt-front migration. Similar to previous studies, one of the findings of the proposed method is the linear relationship between melt-front depth and square root of time, as in Figure 2a. With the same period of time, the estimated migration of the melt front from the proposed method is compared with those of the Stefan model, Neumann solution and "modified Berggren Equation". At all the time steps the proposed model has a slower thaw front migration than the comparative models, by 18.5%, 12.0% and 4.3%; respectively.

In Figure 2b, for the given scenario, with the given 1-meter vertical pipe heated at top surface with a constant temperature of 40℃, after 25 days the depth of the melt front reaches 54.3 cm, 50.3 cm, and 46.2 cm when using conventional Stefan model, Neumann solution and "modified Berggren equation", respectively; while for the proposed method, it was 44.2 cm.

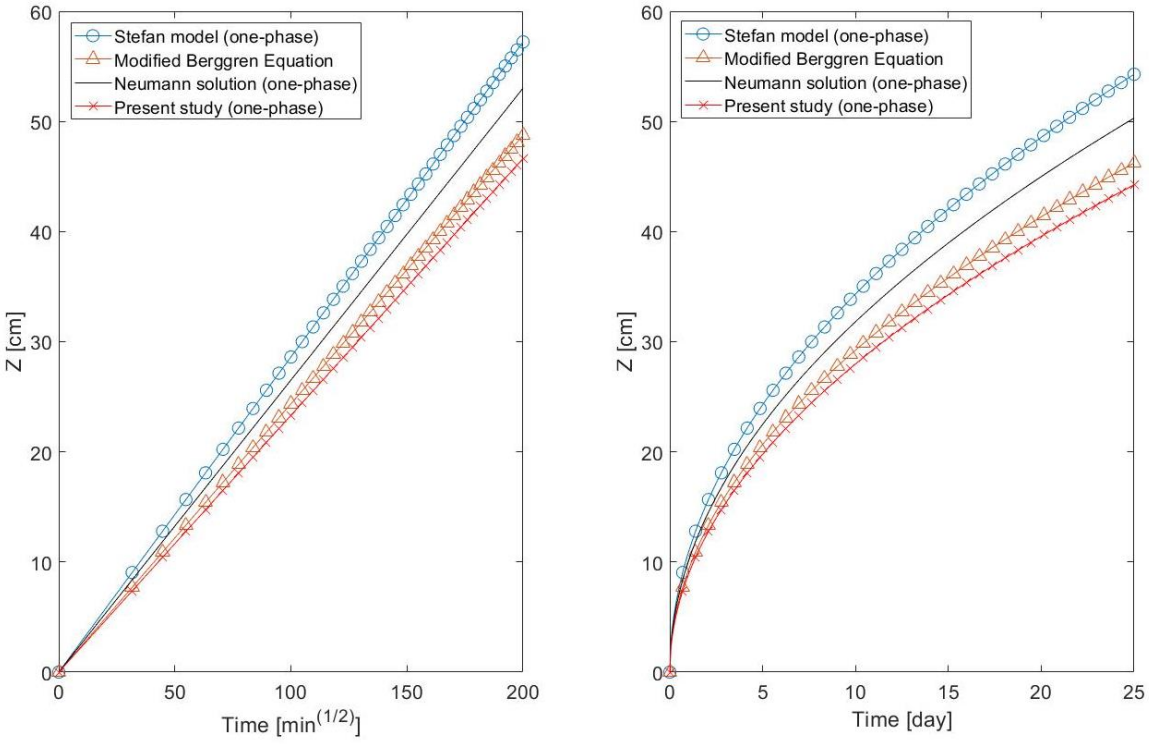

(a) (b)

Figure 2. Melt-front migration with time in $min^{1/2}$ (a); and day (b) for one-phase case.

The conventional one-phase Stefan model was shown to be the fastest one among all the cases. By considering sensible heat of the liquid phase using analytical Neumann solution and a correction factor of "modified Berggren Equation", the solution has improved mathematically. By not omitting the sensible heat term due to mathematical technique, i.e., Eq. (24) instead of Eq. (15), the proposed model showed a comparable result to previous studies.

3.1.2. Two-phase models

For the two-phase case, the Stefan model, Rodrıguez-Aleman et al. (2020) and our proposed model are observed to have a similar trend, in which the melt-front positions are non-linear to the square root of time (Figure 3a). The Stefan model gave the fastest thaw front migration rate, next comes the Rodrıguez-Aleman et al. (2020), and the proposed model is the slowest one. The deviation of the Rodrıguez-Aleman et al. (2020) and the proposed model, compared to the Stefan model, increases after a certain period and remains stable following this point. In this scenario, after 12 days, the differences were about 2% and 11%, respectively; and remains stable to the end of the simulation period. Rodriguez-Aleman et al. (2020) and the proposed model provided a slower migration-rate than that of the Stefan model since they include additional physical phenomena. However, in this specific instance, the net sensible heat of the phases dominates the effect of volume change.

On the other hand, the result from the model of Kurylyk and Hayashi (Kurylyk and Hayashi 2016), which consider non-zero initial temperature, showed a linear relationship between melt-front position and square root of time (Fig. 3a). At the beginning of the melting process, the migration of the interface from the proposed model was closer to the study of Kurylyk and Hayashi. However, after a certain period, around 10 days in this scenario, the migration rate of Kurylyk and Hayashi was faster than that of the two-phase Stefan model (Figure 3b). This results from the fact that their model was derived from the one-phase model (Kurylyk and Hayashi 2016). Meanwhile, the proposed model was consistently lower than the Stefan model. We observe that initial temperature (Kurylyk and Hayashi 2016) and net sensible heat (present study) have slowed down the interface migration compared to the volume change effect of Rodrıguez-Aleman et al. (2020) at the beginning of the thawing process. As time went on the consequences of the volume change on the melting process steadily grew. Meanwhile, by including the net sensible heat of the phases, the proposed model was found to maintain its effect by slowing down the migration of the interface by a stable rate compared to the conventional Stefan model.

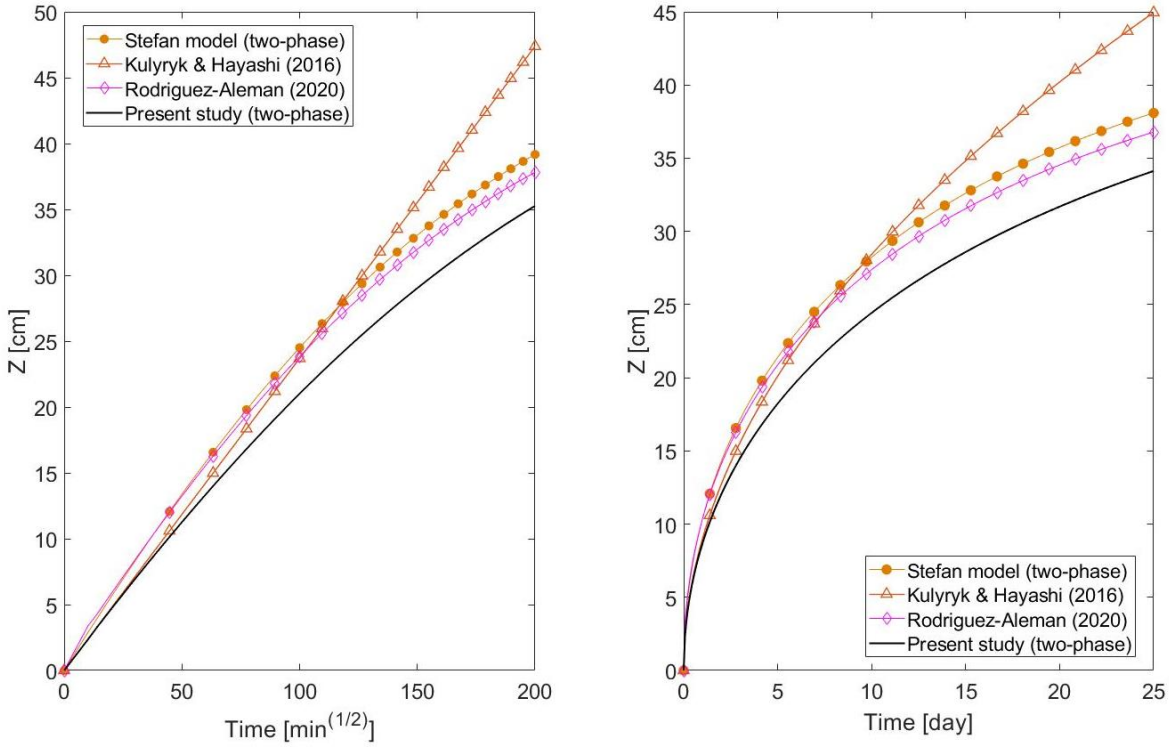

Figure **3**. *Melt-front migration with time in min$^{1/2}$ (a); and day (b) for two-phase case.*

3.1.3. One-phase and two-phase comparison

Figure 4 shows the results of Kurylyk and Hayashi, the Neumann solution, the "modified Berggren Equation", Rodriguez-Aleman and both the one-phase and two-phase cases of Stefan's and the proposed models. In general, the interface positions of the one-phase cases were observed to grow faster than those of the two-phase cases. In all models, as time increased, the effect of adding a solid phase to the equations was that the melting process was affected considerably.

With the given input values, to melt ice to 30-cm depth, the Stefan two-phase case takes 55% longer than that of the Stefan one-phase case, i.e., 11.8 days compared to 7.6 days. Likewise, for the proposed model, the difference was 49%, i.e., 17.2 days for two-phase compared to 11.5 days for one-phase. As the difference between the Stefan one-phase Eq. (15) and two-phase Eq. (17a) is the addition of the solid phase, the heat flux into the solid phase affects the melt-front migration by slowing it down; this also happens to our proposed methods in Eq. (24) and Eq. (25). Meanwhile, other results are in between the Stefan models and our proposed models for both the one-phase and two-phase cases.

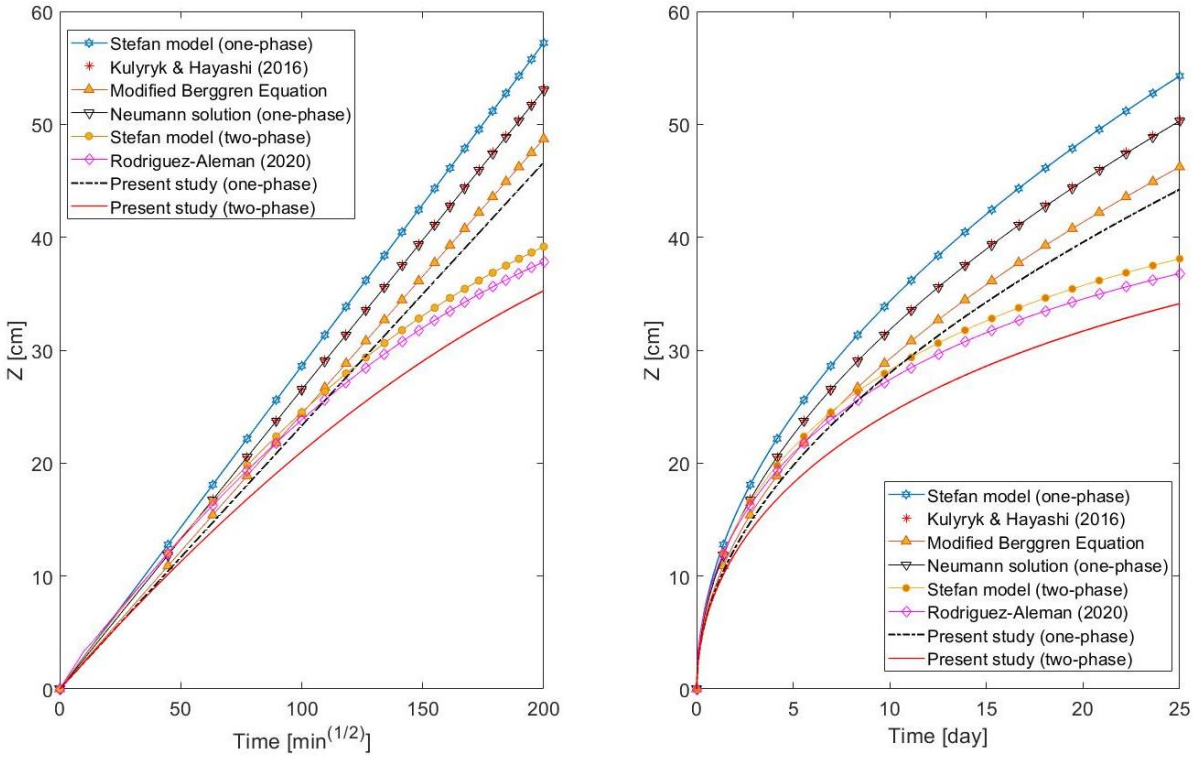

(a) (b)

Figure **4***. Melt-front migration with time for one-phase and two-phase cases in* $min^{1/2}$ *(a); and day (b).*

Unlike Stefan's models in which sensible heat of each phase has been omitted, Eq. (10), in the proposed models, the net-sensible-heat of the liquid and solid phases are included in the two-phase case, Eq. (22), while only the sensible heat of the liquid phase was included for the one-phase case, Eq. (23). As in Figure 5a, the net rate of sensible heat is also the sensible heat of the liquid as the solid phase is negligible in one-phase cases. On the other hand, in Figure 5b, those of both liquid and solid phases were demonstrated for the two-phase case; in which, sensible heat of the liquid phase is greater than that of the solid phase. Therefore, the net sensible heat is of considerable importance in the estimation of the melt-front interface.

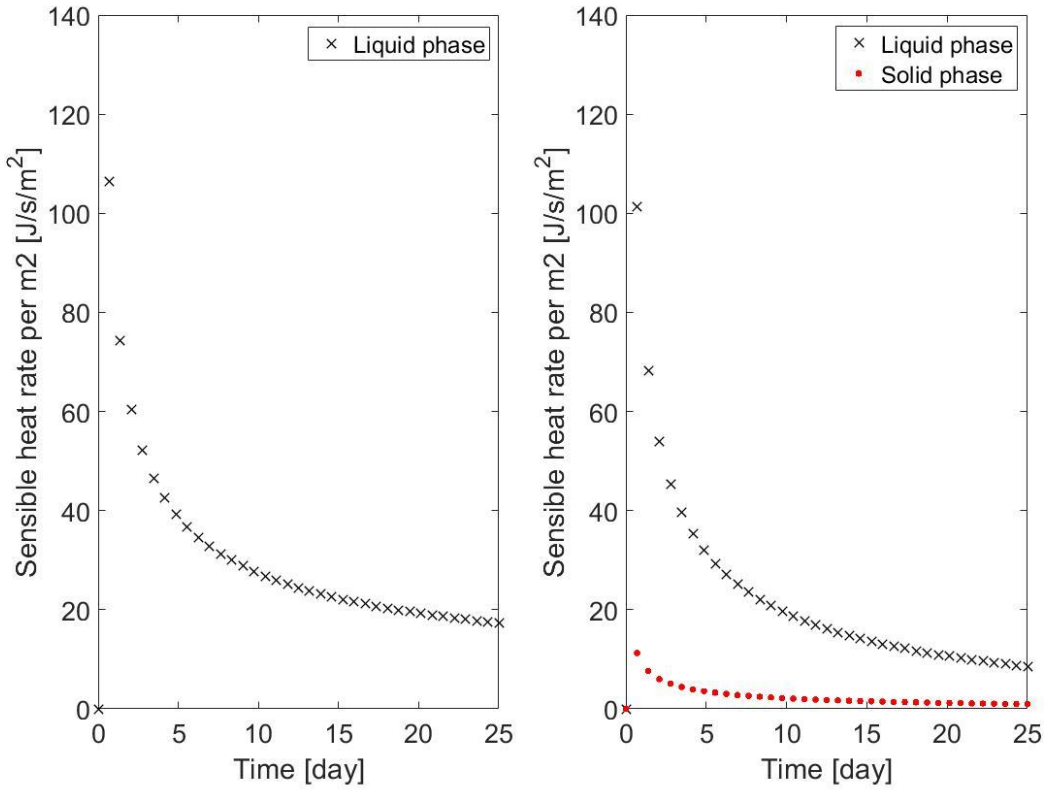

(a) One-phase case (Eq. 23) (b) Two-phase case (Eq. 22)

Figure 5. Sensible heat rate (per m^2) for (a) one-phase and (b) two-phase cases of proposed models.

3.2 Sensitivity analysis of the proposed model

With the purpose of evaluating the robustness of the proposed method, a sensitivity analysis can help to identify uncertain input values which have significant impact on the melt-front migration, based on Eq. (24) for one-phase and Eq. (25) for two-phase cases. In the present model, the density ρ, conductivity λ and heat capacity c of each phase are assumed to be unchanged and whose values are in Table 1. It is noted that non-dimensional Stefan number, which is ratio of sensible heat to latent heat, is not included since the model is not limited for certain Stefan numbers. The varied physic-parameter inputs are surface temperature T_0, initial temperature T_i and pipe length l.

a. Effects of surface temperature T_0

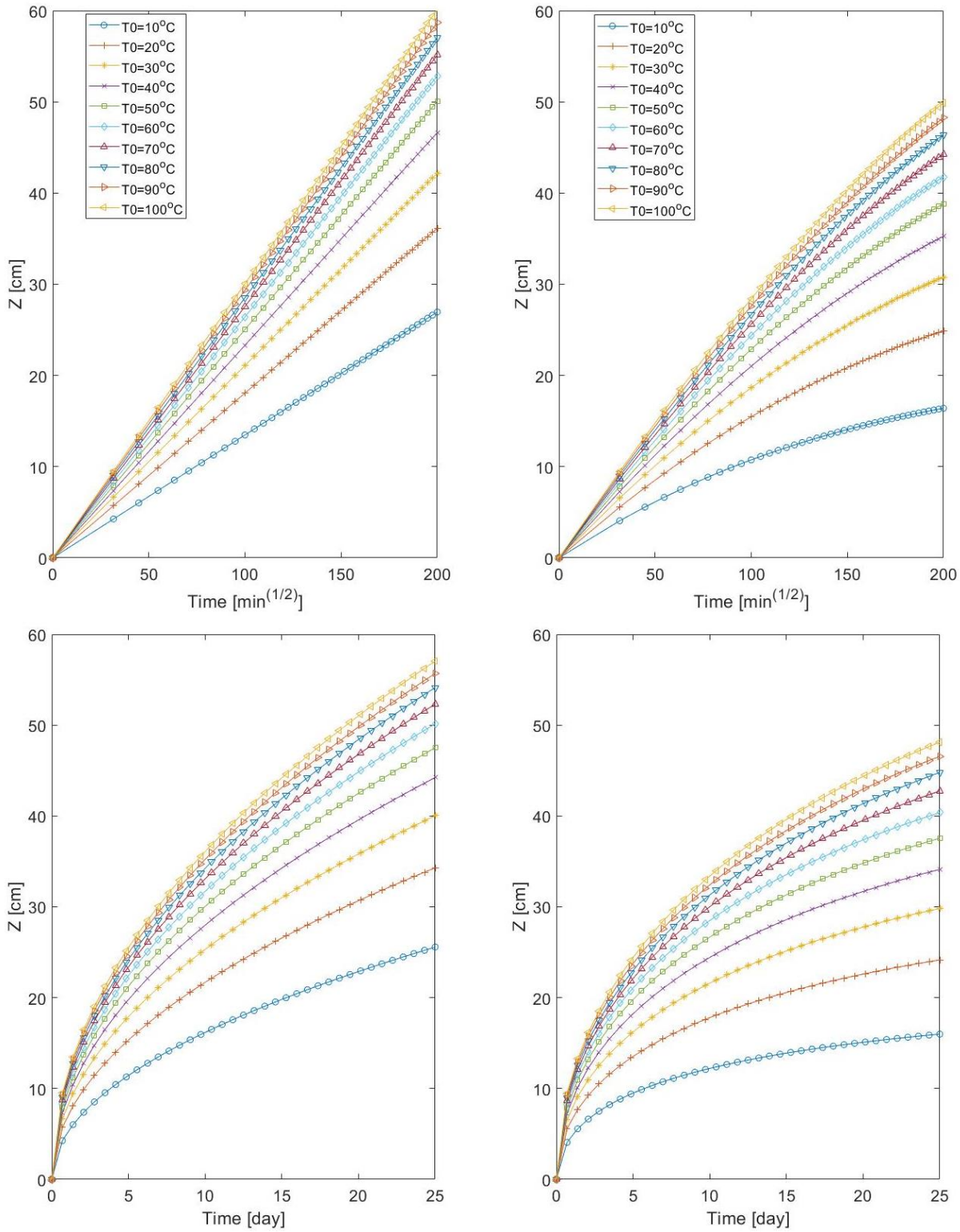

(a) one-phase (Eq. 24) (b) two-phase (Eq.25)

Figure **6**. *Interface position change with time and varying* T_0 *in the range of 10°C to 100°C.*

By keeping pipe length at $l = 1.0m$ and temperature at $T_l = -10$℃, Figure 6 revealed that as T_0 increases, the migration of the interface is faster. Specifically, after 25 days of melting, for $T_0 = 10$℃, the depth of liquid reached 25.6 cm for the one-phase case, while it was 16 cm for the two-phase case; on the other hand, for $T_0 = 100$℃, they are 57 cm and 48.1 cm, respectively for one- and two-phase cases. In addition, the graph shows that even if temperature difference is fixed with 10°C, the rate of migration of the interface decreased as the surface temperature increased. For instance, for the two-phase case, after 25 days, as T_0 from 10 ℃ to 20 ℃, the difference in *Z(t)* is about 8.2 cm, whereas T_0 from 90℃ to 100℃, its difference is about 1.56 cm. The reason for this is due to the existence of the net sensible heat inside the pipe, as in Eqs. (24) and (25). Thus, net sensible heat is a significant parameter that affects the melting process.

b. Effects of initial temperature T_i

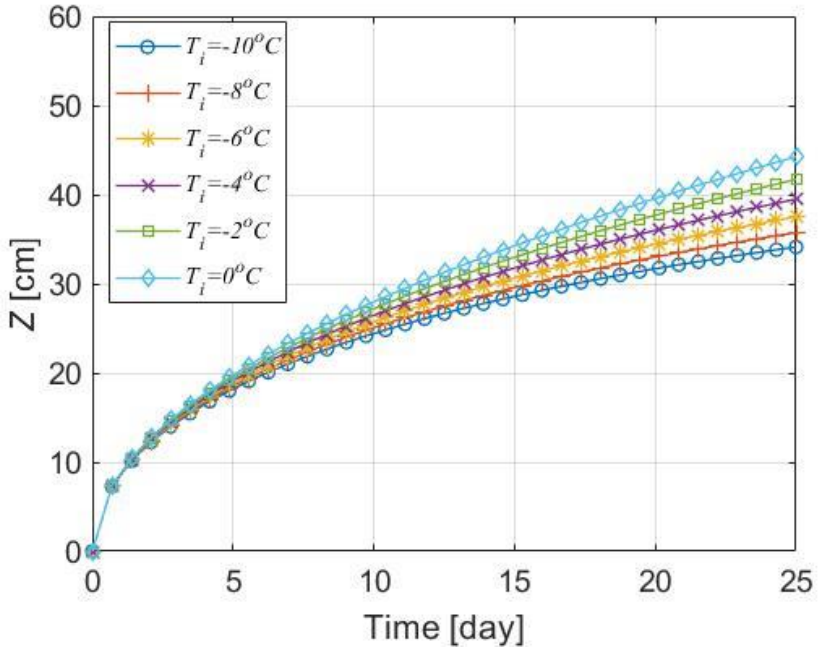

Figure 7. *Interface position change with time for two-phase case as T_i in the range of* −10℃ *to* 0℃.

In the one-phase case, the solid phase is assumed to have no effect on the melting process. Hence, the initial temperature T_i does not affect the interface condition. In contrast, it has great effects on the two-phase case. Figure 7 shows that as the initial temperature of the ice T_i increases from −10℃ to 0℃, after 25 days, the interface migrated about 10.1 cm further than for the two-phase case, while they are the same for the one-phase case. This is due to the larger sensible heat in the solid phase required to heat up the ice to its melting temperature from lower-than-melting temperature. In addition, at $T_0 = 0$℃, it agrees well with the Neumann solution (Alexiades and Solomon 1993), as Z(t) developed linearly with square root of time.

The rate of melting is proportional to square root of cumulative time as the surface temperature is constant (Kurylyk and Hayashi 2016). The coefficient of proportionality, $Z/\sqrt{t}[\text{cm} \cdot (min)^{-0.5}]$, is considered as the rate of migration of the melting interface *Z* with respect to the square-root-of-time. In the one-phase case, this coefficient is constant, as seen in Figure 2a; while for the two-phase case, it depends on the thermal properties of solid and liquid, initial temperature or temperature difference between the initial temperature and melting temperature and the latent heat during the phase change (Kurylyk and Hayashi 2016).

In order to generalize the proposed model compared to other models in the literature, the coefficients of proportionality of the two-phase cases are shown in graphs in Figure 8. In this figure, $\Delta T_i = T_m - T_i$ is the temperature difference between the initial temperature and the melting temperature; and $\Delta T_0 = T_0 - T_m$ is the temperature difference between the surface heating temperature and the melting temperature.

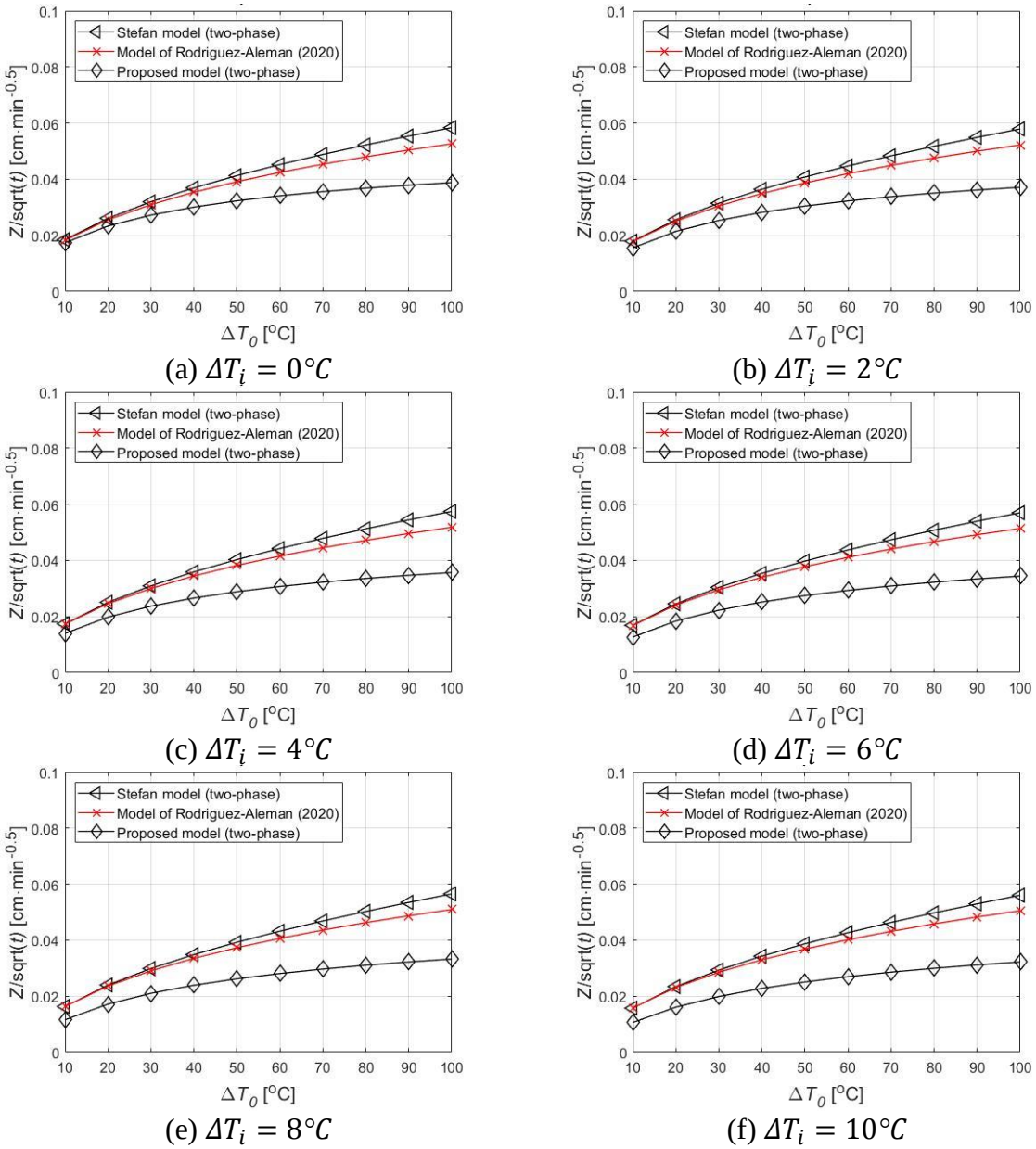

(a) $\Delta T_i = 0°C$ (b) $\Delta T_i = 2°C$

(c) $\Delta T_i = 4°C$ (d) $\Delta T_i = 6°C$

(e) $\Delta T_i = 8°C$ (f) $\Delta T_i = 10°C$

Figure **8**. Comparison of the coefficients of proportionality of the two-phase cases as ΔT_0 and ΔT_i change.

By considering the effects of additional physical parameters of the solid phase to the rate of melting process, both the studies of Rodriguez-Aleman (Rodriguez-Aleman 2020) and our proposed model have shown their effects on the migration of the thawing interface compared to the Stefan model.

- In Stefan model, the only parameter that contributed to the phase change process is the net heat flux applied. As a result, when ΔT_0 increases at a certain initial temperature, which also means that the net heat-flux increases; the melting rate also increases considerably. On the other hand, the lower the initial temperature, the slower melting rate.
- The model of Rodriguez-Aleman (Rodriguez-Aleman 2020) has a trend similar to the Stefan model as ΔT_0 increases, but at a slower rate. It is also observed that the difference in melting rate between this and the Stefan model is getting lower as ΔT_0 increases. For instance, at $\Delta T_0 = 10^o C$, the melting rate difference of the two was 1%; while at $\Delta T_0 = 100^o C$, it was 10%. Meanwhile, the effect of ΔT_i is negligible for this scenario.

- On the other hand, by accounting for the net sensible heat of both phases to the Stefan model, Eq. (22) compared to Eq. (13), the melting rate of the proposed model also showed a similar trend to Stefan model as ΔT_0 increases at certain initial temperature, but at a slower rate. It was also observed that this melting rate difference increased as ΔT_0 increased. For instance, at $\Delta T_i = -10°C$, with $\Delta T_0 = 10^oC$, the melting rate difference was nearly 33%; while with $\Delta T_0 = 100^oC$, it was approximately 43%. Similarly, the melting rate of the proposed model is lower than that of the Stefan model at a certain ΔT_0. For instance, at $\Delta T_0 = 10^oC$, with $\Delta T_i = 0^oC$, the melting rate difference was about 6%; while with $\Delta T_i = 10^oC$, it was nearly 33%.

c. Effects of pipe-length l

In order to investigate the effects of the pipe-length on the proposed model for both one-phase and two-phase cases, the pipe length was varied between 0.60 m, 0.80 m, 1.20 m, and 1.40 m while the other physic-parameter inputs are kept constant. Then, they were compared with the above 1-meter pipe-length results as the time of investigation is extended comparing to Figure 2 and Figure 3. The result showed that, for the one-phase case, the change in pipe-length does not affect the migration of the interface, as in Figure 9a. On the other hand, as pipe-length increases, a slightly higher rate of interface migration was observed for the two-phase case, Figure 9b. In addition, there was a discontinuity after a certain period of time for each pipe-length. Furthermore, the longer pipe-length, the longer the time-period the discontinuity lasted.

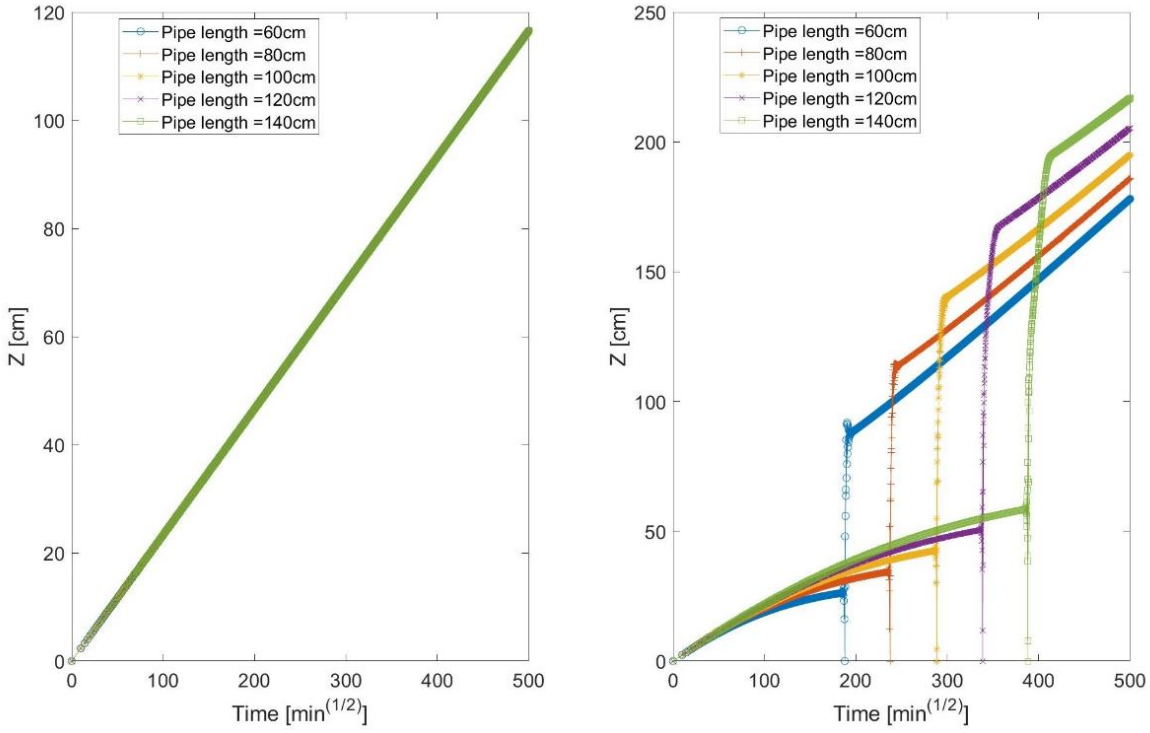

(a) one-phase case (b) two-phase case

Figure **9**. *Interface position change with time and pipe length in the range of 60cm to 140cm.*

In relation to the conservation of energy for each phase, Eq. (1) for liquid and Eq. (2) for solid, the net heat flux on the right-hand side decides the change of enthalpy with time in the control volume of each phase inside the pipe. Hence, in this case the net heat flux is zero; in other words, heat flux in is equal to the heat flux out of the control volume, there is no longer a change in enthalpy with time. Thus, for this special case, the right-hand side of Eq. (13) for the Stefan model and Eq. (22) for the proposed model are zero. Consequently, this is the limitation of both the Stefan and the proposed models for the two-phase case as the net heat-flux reaches non-positive value.

For different pipe-lengths, Figs. 10 (b) and (d) demonstrated that at the time the net heat-flux reaches zero, the discontinuity of *Z(t)* occurred as in Figs. 10 (a) and (c) for both the Stefan's and the proposed models. However, with the same pipe-length, it took a longer time to reach discontinuity point than that of the Stefan model. To demonstrate, at pipe-lengths of 0.6m, 0.8m, 1.0m, 1.2m and 1.5m, the time differences are 6.5 days, 11.9 days, 17.2 days, 25.6 days,

and 32.9 days, respectively. The delay occurs because of the existence of the sensible heat of each phase in the proposed model.

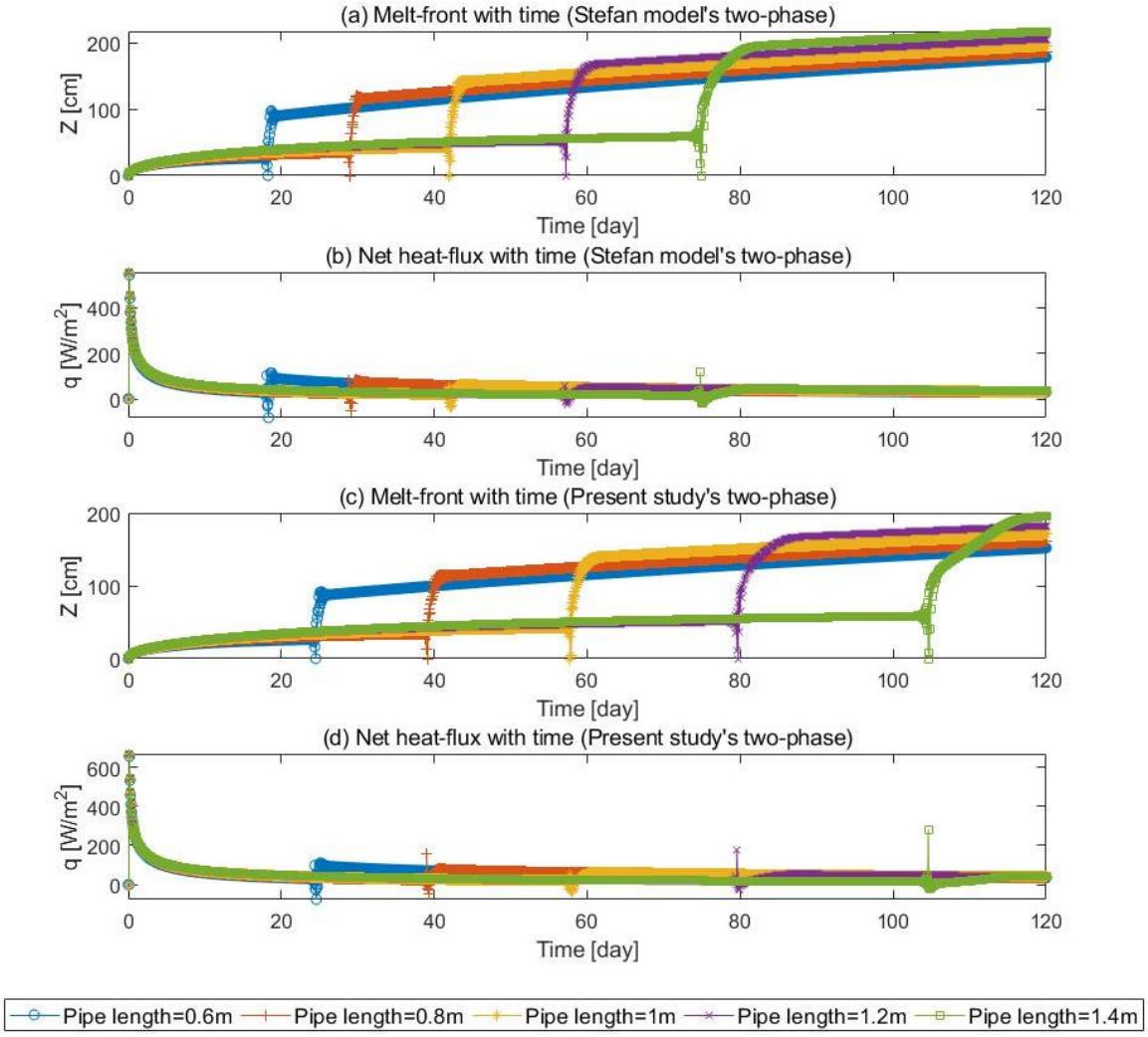

Figure **10.** *Interface position and net heat flux as the pipe length changes.*

3.3 Validity and application of the proposed model

It has been shown in previous studies that the simplifications made to derive the Stefan model tend to bias the model by increasing the freezing and melting rates (Leppäranta 1993). The net sensible heat in both one-phase and two-phase cases has a significant effect on the melt-front migration. From the above results, the proposed models for evaluating the melt-front migration are also comparable with many other models (Alexiades and Solomon 1993, Kurylyk and Hayashi 2016).

Validity of the proposed model

As mentioned above, the validity of the proposed model is quite similar to the Stefan model for a semi-infinite pipe length, for both one-phase and two-phase cases. In detail, if the length of the pipe is limited, the discontinuity happens after a certain period for a given initial set of physic-parameters. From Eqs. (24) and (25), the proposed model is valid if the terms under the square root are fulfilled. Since $t > 0$, $T_0 > T_m$, Eq. (24) for the one-phase model this is always satisfied. On the other hand, Eq. (24) for two-phase is satisfied as long as:

$$\beta > \frac{\lambda_s(T_m - T_l)}{\lambda_L(T_0 - T_m)} \text{ and } \rho_L L + c_L \rho_L \Delta T_L - c_s \rho_s \Delta T_s > 0 \quad (26)$$

In the melting processes, the rate of migration of the melt-front interface must be positive; thus,

$$\frac{\partial Z(t)}{\partial t} \geq 0$$

Referring to Eq. (22), the remaining term ($\rho_L L + c_L \rho_L \Delta T_L - c_s \rho_s \Delta T_s$) on the left-hand side depends on the net heat flux of the control volume. For that reason, the second term in Eq. (26) is satisfied when the heat flux in greater than heat flux out; therefore, at the melt-front interface:

$$-\lambda_L \frac{T_0 - T_m}{Z(t)} > -\lambda_s \frac{T_m - T_l}{\beta Z(t)} \quad (27)$$

By replacing Eq. (16), it becomes:

$$Z(t) < \frac{\lambda_L(T_0 - T_m)}{\lambda_L(T_0 - T_m) + \lambda_s(T_m - T_l)} l \quad (28)$$

Consequently, as long as the melting distance *Z(t)* satisfies Eq. (28), which has considered other inputs, i.e., length of the pipe, temperature at the end of the pipe and surface temperature, the proposed method is valid.

Applications of the proposed models

The proposed models can potentially be used to evaluate the melting process, when the length of the profile is semi-infinite, and the initial temperature of the ice is able to be obtained or measured. For instance, they can be applied to predict thawing or melting of frozen drainage pipes under roads in arctic conditions (used to prevent ditches on the side of roads filling with water).

Similar to the Stefan model, although the proposed models require additional parameters, i.e. length to melt and temperature at that point, engineers can make use of the proposed model to estimate the required input heat flux or surface temperature and time for melting to a pre-determined length of melting. The proposed model can also be expanded to optimize the varied heat flux or surface temperature in order to achieve a specified melting-depth in the shortest time.

4. CONCLUSIONS

The Stefan model is widely used in estimating melting process because of its simplicity, but the results can lead to over-estimation of the thaw front migration. In this work, we evaluate the complexity at the interface in an ice-melting process in a vertical pipe. As sensible heat of the phases, which is an important physic effect of the melting process, were omitted in the energy conservation equation in the Stefan models, the proposed models have included sensible heat by combining energy conservation equations in differential form. The findings are as follow:

- The results gave comparable outcomes to other related studies in predicting the interface position. Compared to other similar studies for the one-phase case, the trend of melting pattern is quite similar. The proposed model has a reduction in thaw front migration rate by 18.5%, 12.0% and 4.3% compared to those of the Stefan model, Neumann solution and "modified Berggren Equation," respectively, after 25 days for the given scenario. For the two-phase case, the trend was similar for the proposed study and that of the Stefan's model with a reduction of approximately 11.4% lower after about 12 days, this difference remains stable for the rest of the simulation period.
- By applying Equation (24) instead of Equation (15) for the one-phase case and Equation (25) instead of Equation (17a) for the two-phase case, the study has offered an easily-implemented methodology, as simple as the Stefan models.
- As the initial temperature, surface temperature and length of the pipe changed, the proposed model showed good agreement to previous models for both one-phase and two-phase cases.

Even though the proposed models need to be verified by future experimental work, it can still be used as an alternative model for engineers to evaluate the melting process, where length and temperature are measurable.

Nomenclature

T: Temperature, K

T_m: Melting temperature, K

T_0: Temperature on the surface, K

T_l: Temperature at the end of the pipe, K

T_i: Initial temperature of the pipe, K

λ_L, λ_s: Thermal conductivity of the liquid and solid phase, respectively, $\mathrm{W/m \cdot K}$

c_L, c_s: Specific heat capacity of the liquid and solid phase, respectively, $\mathrm{J/kg \cdot K}$

ρ_L, ρ_s: Density of liquid and solid phase respectively, $\mathrm{kg/m^3}$

L: Specific latent heat of fusion, $\mathrm{J/kg}$

A: Cross section area, $\mathrm{m^2}$

l: Pipe length, m

m_L, m_s: Mass of liquid and solid phase, respectively, kg

t: Time, min or day

b: geometric parameter

ΔT_L, ΔT_s: increase of temperature in the liquid and solid phases, respectively, K

Subscript:

L, s: liquid and solid, respectively

REFERENCES

1. Alexiades, V., and Solomon, A.D. 1993. Mathematical modelling of melting and freezing processes. Washington, USA: Hemisphere.
2. Sveen, S. E., Nguyen, H. T., and Sørensen, B. R. (2017). "Thaw penetration in frozen ground subjected to hydronic heating." J. Cold Reg. Eng., 10.1061/(ASCE)CR.1943-5495.0000117:31(1).
3. David E. Glass, M. Necati Ozisik, S. Scott McRae, and W. S. Kim. 1991 Formulation and solution of hyperbolic Stefan problem. J. Appl. Phys 70, 1190. https://doi.org/10.1063/1.349572
4. Berggren, W.P. 1943. Prediction of temperature- distribution in frozen soils. Eos Trans. AGU, 24(3), 71–77, https://doi.org/10.1029/TR024i003p00071.
5. Cannon, J.R., Di Benedetto, E., and Knightly G.H. 1980. The steady state Stefan problem with convection. Arch. Rational Mech. Anal. 73, 79–97. https://doi.org/10.1007/BF00283258.
6. Cengel Y. Heat and Mass Transfer: A Practical Approach. 3rd ed. McGraw-Hill Science/Engineering/Math.2006

7. Changwei, X., and Gough, W.A. 2013. A Simple Thaw-Freeze Algorithm for a Multi-Layered Soil using the Stefan Equation. Permafrost and Periglac. Process. 24, 252-260. https://doi.org/10.1002/ppp.1770.
8. Charach, Ch., and Rubinstein, I. 1991. Pressure-temperature effects in planar Stefan problem with density change. J. Appl. Phys. 71 (3) https://doi.org/10.1063/1.351277.
9. French, H.M. 2007. The periglacial environment, 3rd ed. West Sussex, England: John Wiley and Sons Ltd.
10. Fox, J.D. 1992. Incorporating Freeze-Thaw Calculations into a Water-Balance Model. Water Resources Research, 28, 2229-2244.
11. Hayashi, M., Goeller, N., Quiton, W.L., and Wright N. 2007. A simple heat- conduction method for simulating the frost-table depth in hydrological models. Hydrol. Process. 21, 2610-2622. https://doi.org/10.1002/hyp.6792.
12. Jumikis, A.R. 1977. Thermal Geotechnics. New Brunswick, USA: Rutgers University Press.
13. Kurylyk, B.L. 2015. Discussion of 'A Simple Thaw- Freeze Algorithm for a Multi- Layered Soil using the Stefan Equation' by Xie and Gough (2013). Permafrost and Periglac. Process., 26, 200– 206. https://doi.org/10.1002/ppp.1834.
14. Kurylyk, B.L., and Hayashi, M. 2016. Improved Stefan equation correction factors to accommodate sensible heat storage during soil freezing or thawing. Permafrost and Periglac. Process. 27, 189-203. https://doi.org/10.1002/ppp.1865.
15. Kurylyk, B.L., McKenzie, J.M., MacQuarrie, K.T.B., and Voss, C.I. 2014. Analytical solutions for benchmarking cold regions subsurface water flow and energy transport models: One-dimensional soil thaw with conduction and advection. Adv. Water Resource. 70, 172-184. https://doi.org/10.1016/j.advwatres.2014.05.005.
16. Leppäranta, M. 1993. A review of analytical models of sea-ice growth. Atmosphere-Ocean, DOI: 10.1080/07055900.1993.9649465
17. Li, X., Otsuka, N., Brigham, L.W. 2021 Spatial and temporal variations of recent shipping along the Northern Sea Route, Polar Science, Volume 27 https://doi.org/10.1016/j.polar.2020.100569.
18. Neumann F. C. 1860. Lectures given in the 1860's, cf. Riemann-Weber, Die Partiellen Differentialgleichungen der Mathematischen. Physik 2: 117–121.
19. Stefan, J. 1889a. Über einige problem der theorie der wärmeleitung. [In German] Sitzungsberichte der Österreichischen Akademie der Wissenschaften Mathematisch- Naturwissenschaftliche Klasse, Abteilung 2, Mathematik, Astronomie, Physik, Meteorologie und Technik, 98, 473-484.
20. Stefan, J. 1889b. Über die Diffusion von sauren und basen gegen einander. [In German] Sitzungsberichte der Österreichischen Akademie der Wissenschaften Mathematisch- Naturwissenschaftliche Klasse, Abteilung 2, Mathematik, Astronomie, Physik, Meteorologie und Technik, 98, 616-634.
21. Stefan, J. 1889c. Über die Theorie der Eisbildung, insbesondere über die Eisbildung im polarmeere. [In German] Sitzungsberichte der Österreichischen Akademie der Wissenschaften Mathematisch-Naturwissenschaftliche Klasse, Abteilung 2, Mathematik, Astronomie, Physik, Meteorologie und Technik, 98, 965-983.
22. S. Rodríguez-Alemán, E.M. Hernández-Cooper and J.A. Otero, Consequences of Total Thermal Balance during Melting and Solidification of High Temperature Phase Change Materials, Thermal Science and Engineering Progress (2020), doi: https://doi.org/10.1016/j.tsep.2020.100750
23. Stefan, J. 1889d. Über die Verdampfung und die Auflösung als Vorgange der diffusion. [In German] Sitzungsberichte der Österreichischen Akademie der Wissenschaften Mathematisch- Naturwissenschaftliche Klasse, Abteilung 2, Mathematik, Astronomie, Physik, Meteorologie und Technik, 98, 965-983
24. Tao, L.N. 1979. On Solidification problems including the density jump at the moving boundary. Q. J. Mech. Appl. Math., 10 pp.
25. Xuejing Deng, Shaowei Pan, Zhiyuan Wang, Ke Ke, and Jianbo Zhang. 2019. Application of the Darcy-Stefan model to investigate the thawing subsidence around the wellbore in the permafrost region, Applied Thermal Engineering, Volume 156, 2019, Pages 392-401, ISSN 1359-4311, https://doi.org/10.1016/j.applthermaleng.2019.04.042.
26. Crepeau, J., and Siahpush, A. S. 2012. Solid–liquid phase change driven by internal heat generation. Comptes Rendus Mécanique, 340(7), 471–476. https://doi.org/10.1016/j.crme.2012.03.004.
27. An, C., and Su, J. 2013. Lumped parameter model for one-dimensional melting in a slab with volumetric heat generation. Applied Thermal Engineering, 60(1-2), 387–396. https://doi.org/10.1016/j.applthermaleng.2013.07.018.

28. S. H. Chan and K. Y. Hsu. 1987. Generalized phase change model for melting and solidification with internal heat generation. Journal of Thermophysics and Heat Transfer 1987 1:2, 171-174.